†J.J.M. and J.A.T. are joint senior authors.

The data reported in this article have been deposited in the European Genome-phenome Archive database (accession number EGAS00001003511) at https://ega-archive.org/studies/EGAS00001003511.

The online version of this article contains a data supplement.

REFERENCES

1. Voskoboinik I, Whisstock JC, Trapani JA. Perforin and granzymes: function, dysfunction and human pathology. *Nat Rev Immunol*. 2015;15(6):388-400.
2. Stepp SE, Dufourcq-Lagelouse R, Le Deist F, et al. Perforin gene defects in familial hemophagocytic lymphohistiocytosis. *Science*. 1999;286(5446): 1957-1959.
3. Clementi R, Locatelli F, Dupré L, et al. A proportion of patients with lymphoma may harbor mutations of the perforin gene. *Blood*. 2005; 105(11):4424-4428.
4. Voskoboinik I, Dunstone MA, Baran K, Whisstock JC, Trapani JA. Perforin: structure, function, and role in human immunopathology. *Immunol Rev*. 2010;235(1):35-54.
5. Molleran Lee S, Villanueva J, Sumegi J, et al. Characterisation of diverse PRF1 mutations leading to decreased natural killer cell activity in North American families with haemophagocytic lymphohistiocytosis. *J Med Genet*. 2004;41(2):137-144.
6. Mancebo E, Allende LM, Guzmán M, et al. Familial hemophagocytic lymphohistiocytosis in an adult patient homozygous for A91V in the perforin gene, with tuberculosis infection. *Haematologica*. 2006;91(9): 1257-1260.
7. Zhang K, Chandrakasan S, Chapman H, et al. Synergistic defects of different molecules in the cytotoxic pathway lead to clinical familial hemophagocytic lymphohistiocytosis. *Blood*. 2014;124(8):1331-1334.
8. Chia J, Yeo KP, Whisstock JC, Dunstone MA, Trapani JA, Voskoboinik I. Temperature sensitivity of human perforin mutants unmasks subtotal loss of cytotoxicity, delayed FHL, and a predisposition to cancer. *Proc Natl Acad Sci USA*. 2009;106(24):9809-9814.
9. Mehta PA, Davies SM, Kumar A, et al; Children's Oncology Group. Perforin polymorphism A91V and susceptibility to B-precursor childhood acute lymphoblastic leukemia: a report from the Children's Oncology Group. *Leukemia*. 2006;20(9):1539-1541.
10. Cappellano G, Orilieri E, Comi C, et al. Variations of the perforin gene in patients with multiple sclerosis. *Genes Immun*. 2008;9(5):438-444.
11. Vastert SJ, van Wijk R, D'Urbano LE, et al. Mutations in the perforin gene can be linked to macrophage activation syndrome in patients with systemic onset juvenile idiopathic arthritis. *Rheumatology (Oxford)*. 2010;49(3): 441-449.
12. Trambas C, Gallo F, Pende D, et al. A single amino acid change, A91V, leads to conformational changes that can impair processing to the active form of perforin. *Blood*. 2005;106(3):932-937.
13. Voskoboinik I, Sutton VR, Ciccone A, et al. Perforin activity and immune homeostasis: the common A91V polymorphism in perforin results in both presynaptic and postsynaptic defects in function. *Blood*. 2007;110(4): 1184-1190.
14. Voskoboinik I, Trapani JA. Perforinopathy: a spectrum of human immune disease caused by defective perforin delivery or function. *Front Immunol*. 2013;4:441.
15. McNeil JJ, Nelson MR, Woods RL, et al; ASPREE Investigator Group. Effect of aspirin on all-cause mortality in the healthy elderly. *N Engl J Med*. 2018; 379(16):1519-1528.
16. McNeil JJ, Wolfe R, Woods RL, et al; ASPREE Investigator Group. Effect of aspirin on cardiovascular events and bleeding in the healthy elderly. *N Engl J Med*. 2018;379(16):1509-1518.
17. McNeil JJ, Woods RL, Nelson MR, et al; ASPREE Investigator Group. Baseline characteristics of participants in the ASPREE (Aspirin in Reducing Events in the Elderly) study [published correction appears in J Gerontol A Biol Sci Med Sci. 2019;74(5):748]. *J Gerontol A Biol Sci Med Sci*. 2017; 72(11):1586-1593.
18. McNeil JJ, Woods RL, Nelson MR, et al; ASPREE Investigator Group. Effect of aspirin on disability-free survival in the healthy elderly. *N Engl J Med*. 2018;379(16):1499-1508.
19. Lacaze P, Sebra R, Riaz M, et al. Resilience to dominant genetic disease in the healthy elderly [published online ahead of print 22 October 2019]. *medRxiv*. doi:10.1101/19006932.
20. Trapani JA, Thia KY, Andrews M, et al. Human perforin mutations and susceptibility to multiple primary cancers. *OncoImmunology*. 2013;2(4): e24185.
21. Karczewski KJ, Francioli LC, Tiao G, et al. Variation across 141,456 human exomes and genomes reveals the spectrum of loss-of-function intolerance across human protein-coding genes [published online ahead of print 13 August 2019]. *bioRxiv*. doi:10.1101/531210.

DOI 10.1182/blood.2019003487

TO THE EDITOR:

FER and FES tyrosine kinase fusions in follicular T-cell lymphoma

Koen Debackere,[1-3,*] Jo-Anne van der Krogt,[2,*] Thomas Tousseyn,[4] Julio Antonio Finalet Ferreiro,[2] Katrien Van Roosbroeck,[2] Lukas Marcelis,[4] Carlos Graux,[5] Daan Dierickx,[3] Geneviève Ameye,[2] Peter Vandenberghe,[2,3] Lucienne Michaux,[2] Jan Cools,[1,2] and Iwona Wlodarska[2]

[1]Center for Cancer Biology, Vlaams Instituut voor Biotechnologie, Leuven, Belgium; [2]Center for Human Genetics, Katholieke Universiteit (KU) Leuven, Leuven, Belgium; [3]Department of Hematology, Universitair Ziekenhuis Leuven, Leuven, Belgium; [4]Translational Cell and Tissue Research Laboratory, KU Leuven, Leuven, Belgium; and [5]Mont-Godinne University Hospital, Yvoir, Belgium

Follicular T-cell lymphoma (FTCL) is a rare nodal mature T-cell neoplasm included in a broader category of angioimmunoblastic T-cell lymphoma (AITL) and other nodal lymphomas of T follicular helper (TFH) cell origin by the 2017 World Health Organization classification of tumors of hematopoietic and lymphoid tissues.[1] The atypical, clear, medium-size neoplastic cells display a common TFH phenotype with expression of CD4, CD10, BCL6, PD-1, CXCL13, and ICOS.[2] In contrast to AITL, FTCL is characterized by a follicular growth pattern and lacks the proliferation of high endothelial venules and the extrafollicular expansion of follicular dendritic cells. The molecular pathology of FTCL remains incompletely understood. Up to 40% of FTCLs harbor t(5;9)(q33.3;q22.2) fusing the N-terminal part of the interleukin-2 (IL-2)–inducible T-cell kinase (*ITK*) to the tyrosine kinase domain of *SYK* (the spleen tyrosine kinase).[2-4] The ITK-SYK fusion protein acts as a constitutively active SYK tyrosine kinase with in vitro

and in vivo oncogenic properties.[5,6] Notably, mutations in *TET2*, *DNMT3A*, and *RHOA* recurrently occurring in AITL and other TFH-derived lymphomas[4,7] were recently identified in a few patients with FTCL whose samples were analyzed,[4] underpinning the view that TFH-derived lymphomas represent variants of the same disease.

To obtain additional insight into the molecular pathogenesis of FTCL, we performed cytogenetic and molecular studies of 6 new patients from the University Hospital of Leuven and Université Catholique de Louvain Mont-Godinne, Namur, Belgium. Pathology and clinical records were reviewed. The institutional review board (Commissie Medische Ethiek) of the University Hospital approved this retrospective study and renounced the need for written informed consent (study no. S56035, ML10127: 31/01/2014). The methods used in the study can be found in supplemental Methods (available on the *Blood* Web site).

All tumors were negative for *ITK-SYK*, as demonstrated by an initial fluorescence in situ hybridization (FISH) assay (data not shown). Gene expression profiling by RNA sequencing (RNA-seq) showed that results from FTCL patients clustered together, overlapped with peripheral T-cell lymphoma not otherwise specified, and were different compared with normal lymph nodes and anaplastic large cell lymphoma (Figure 1A). Relevant clinical, pathologic, and genetic data from the patients we reported on are shown in Table 1. Notably, all of them were female, although FTCL shows a slight male predominance.[2] Their ages ranged from 58 to 83 years (mean, 70 years). Representative morphologic and immunophenotypic features of the lymphomas are illustrated in supplemental Figure 1.

The karyotype of patient 1 showed a sole t(1;5)(p34;q21.3). FISH identified involvement of the *FER* gene (5q21.3) (Figure 1B) and revealed that t(1;5)(p34;q21.3) in fact masked a cryptic inv(5)(q21.3q33.3). RNA-seq identified an in-frame fusion of exon 8 of *ITK* (5q33.3) to exon 12 of *FER*. The fusion was confirmed by reverse transcription polymerase chain reaction and Sanger sequencing (Figure 1C). Patient 2 harbored complex numerical and structural rearrangements, as demonstrated by multicolor FISH analysis (Figure 1D). FISH analysis with break-apart probes for 14 candidate protein tyrosine kinase (PTK) genes (supplemental Table 1) neighboring chromosomal rearrangements identified a breakpoint in *FES* at 15q26.1 (Figure 1E). RNA-seq identified an in-frame fusion of exon 24 of *RLTPR* (RGD, leucine-rich repeat, tropomodulin and proline-rich containing protein) at 16q22.1 to exon 11 of *FES*. The t(15;16)(q26.1;q22.1)/*RLTPR-FES* rearrangement was confirmed by reverse transcription polymerase chain reaction and Sanger sequencing (Figure 1F). Molecular cytogenetics and RNA-seq of the remaining 4 patients have not identified any PTK fusion genes. By using RNA-seq data, we analyzed the mutation status of genes that are recurrently mutated in TFH-derived lymphomas (*TET2*, *DNMT3A*, *RHOA*, *IDH2*, *CD28*, *FYN*, and *VAV1*[4,7]). None of them were mutated in patient 1 with *ITK-FER*, whereas patient 2 with *RLTPR-FES* harbored TET2 mutations. The 4 PTK fusion-negative patients carried the *RHOA*^{G17V} and *IDH2*^{R172} mutations as well as *TET2* mutations (Table 1).

Previous studies showed that ITK-SYK and ITK-FER fusions act as constitutive tyrosine kinases. ITK-SYK mimics T-cell receptor (TCR) signaling[6] and both ITK-SYK and ITK-FER phosphorylate STAT3.[8] To determine the oncogenic properties of the novel RLTPR-FES fusion protein, we expressed *RLTPR-FES* in the murine hematopoietic IL-3–dependent Ba/F3 cell line. Upon IL-3 withdrawal, RLTPR-FES conferred growth factor–independent growth, revealing that this fusion protein is constitutively active and supports the proliferation and survival of Ba/F3 cells (Figure 1G). Next, we investigated the ability of NVP-TAE684 (small molecule ATP-competitive ALK/FES inhibitor[9,10]) to inhibit the activity of the RLTPR-FES kinase. Ba/F3 cells transformed by RLTPR-FES responded in a dose-dependent manner to NVP-TAE684 treatment and were slightly less sensitive to the inhibitor than SEC31A-ALK–expressing Ba/F3 cells[11] (Figure 1H). A direct inhibitory effect of NVP-TAE684 on RLTPR-FES kinase activity was confirmed by western blot analysis using phospho-specific antibodies. Furthermore, phosphorylation of STAT3 was reduced upon treatment with NVP-TAE684. There was no effect on phosphorylation of AKT, ERK1/2, and STAT5 (Figure 1I). Immunohistochemistry confirmed high levels of STAT3 phosphorylation in the presence of *RLTPR-FES* and *ITK-FER* in the biopsies (supplemental Figure 2). The heterogeneous tumor composition (supplemental Figure 3A), did not allow the identification of a STAT3 signature in bulk RNA (supplemental Figure 3B; supplemental Table 4). We used CIBERSORTx to impute the expression of STAT3 target genes in CD4$^+$ T cells from bulk RNA (Figure 1J). We confirmed high expression levels of STAT3 target genes in patient 2 (*RLTPR-FES*). This was less evident in patient 1 (*ITK-FER*), but this patient had the lowest ratio of TFH cells over total CD4$^+$ T cells.

FER and FES are the only members of a subfamily of non-receptor PTKs. FER is targeted by at least 3 tumor-related fusions: SSBP2-FER identified in a patient with T-cell acute lymphoblastic leukemia,[12] MAN2A1-FER found in hepatocellular carcinoma and other cancers,[13] and ITK-FER detected in 1 patient with peripheral T-cell lymphoma not otherwise specified.[14] All fusions resulted in aberrant constitutive tyrosine kinase activity of FER, and their oncogenic potential was demonstrated in vitro. In contrast, FES seems to play a dual role in tumorigenesis, acting as an oncogene or a tumor suppressor, depending on the cellular context.[15,16] *RLTPR*, partner of *FES*, codes for proteins involved in cytoskeletal organization and cell migration and is required for CD28 costimulation in T cells.[17] The RLTPR-FES fusion contains the RLTPR homodimerization domain,[18] which is presumably important for the enhanced kinase activity of chimera, because FES oligomerization enhances FES kinase activity.[19]

The occurrence of multiple mutations in patients with FTCL is in line with the proposed model of multistage development of TFH-derived lymphomas.[7] These tumors seem to be driven by 2 types of cooperating mutations: (1) early premalignant (non-lineage impact) mutations affecting genes involved in the regulation of DNA methylation (*TET2*, *DNMT3A*, *IDH2*), which occur in hematopoietic stem cells and confer proliferative advantage, and (2) tumor-specific (lineage impact) mutations targeting genes critical to T-cell biology. TFH differentiation requires sustained TCR signaling, costimulation through ICOS and the IL-21-STAT3 axis.[20] *RHOA* mutations enhance ICOS signaling,[21] and ITK-SYK mimics a TCR signal.[6] *RLTPR-FES* and *ITK-FER* represent genetic hits that hijack STAT3 signaling to drive TFH-derived lymphoma.

Our study supports the critical role of PTK fusion genes in the pathogenesis of FTCL and provides additional evidence that

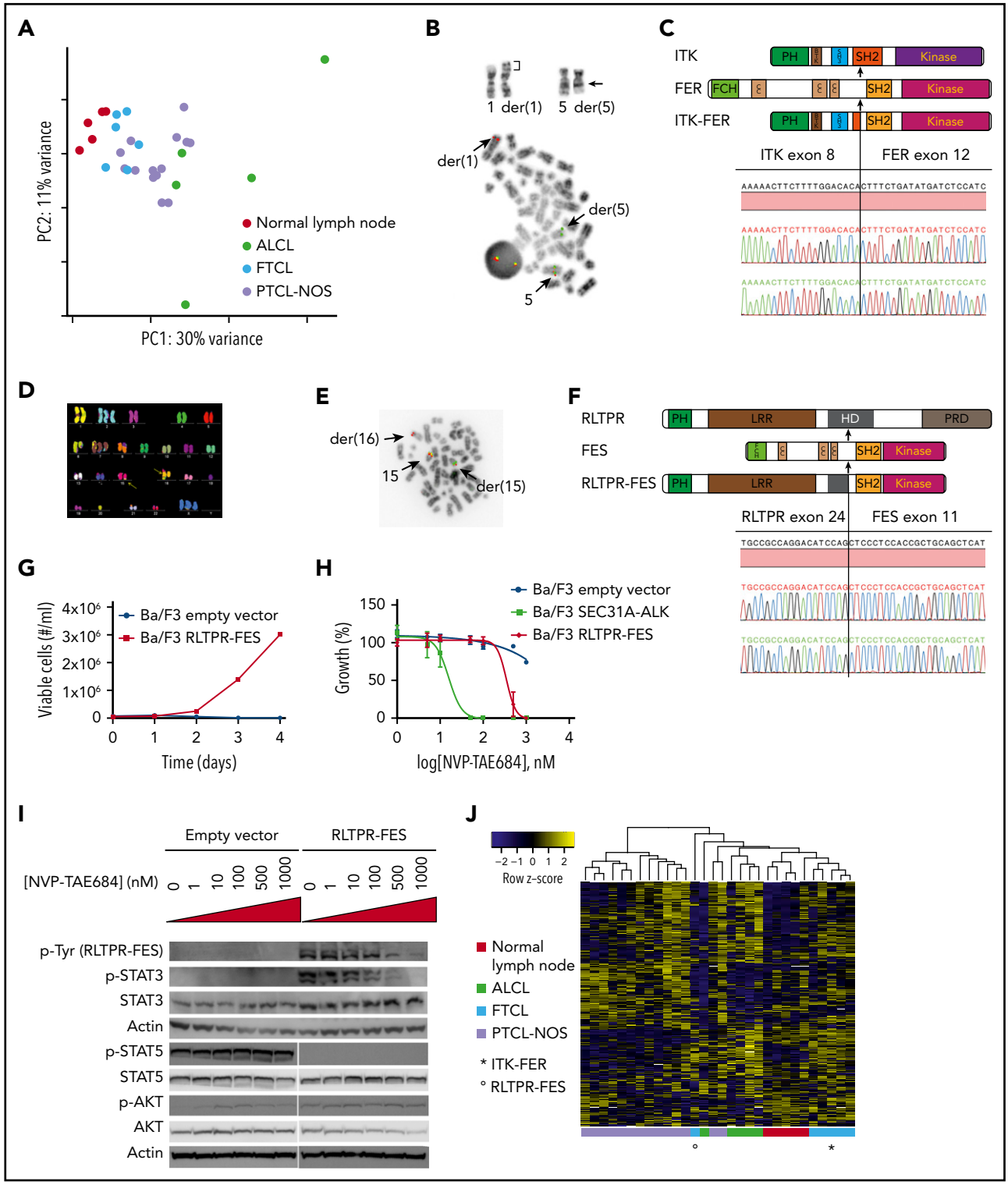

Figure 1. Genetic and functional analysis of the identified fusion genes. (A) Principal component (PC) analysis of gene counts for normal lymph nodes (n = 5), anaplastic large cell lymphoma (n = 5), FTCL (n = 6), and peripheral T-cell lymphoma not otherwise specified (n = 14) using our data and publically available data.[23,24] (B) Partial karyotype illustrating inv(5)(q21q33) masked by t(1;5)(p34;q21) (breakpoints indicated by arrows) identified in patient 1 (upper panel) and metaphase FISH with a dual-color break-apart probe for *FER* (lower panel). (C) Schematic depiction and DNA sequence trace of the *ITK-FER* fusion. (D) Complex karyotype, including cryptic t(15;16)(q26;q22), identified by multicolor FISH in patient 2. (E) Metaphase FISH with a dual-color break-apart probe for *FES* performed in patient 2. (F) Schematic depiction and DNA sequence trace of the *RLTPR-FES* fusion. (G) Growth curve for Ba/F3 cells transduced with either empty vector or *RLTPR-FES*. (H) Relative proliferation of Ba/F3 cells transduced with empty vector, *SEC31A-ALK*, and *RLTPR-FES* in the presence of increasing concentrations of NVP-TAE684. (I) Western blot assessment of phosphorylated tyrosine residues (band at 131 kDa, corresponding to RLPTR-FES), STAT3 phosphorylation, STAT5 phosphorylation, and AKT phosphorylation in Ba/F3 cells transduced with empty vector or RLTPR-FES exposed to increasing concentrations of NVP-TA684. (J) Heat map representing the expression of STAT3 target genes in CD4$^+$ T cells.

Table 1. Clinical, pathological, and genetic features of the patients reported in this study

Patient	Age, y	Immune profile	Sample at diagnosis	Karyotype*	FISH pattern	Mutation status	Stage†	Treatment/ response	Status	Survival, m
1	70	CD4$^+$, CD5$^+$, CD7$^+$, CD10$^+$, BCL6$^+$, PD1 (ICOS and CXCL13: NA), EBER$^+$	Lymph node	46,XX,der(1)(5q35.3→5q33.3::5q21.3→5q33.3::1p34→1q44), der(5)t(1;5)(p34;q21.3)	SYK BA: 2F FER BA: 1F1R1G ITK BA: NI	NF	II	2007: rituximab; CR; 2010/ Rl: rituximab and mini-CHOP; NR; RT/PR; 2011/progression chlorambucil	Dead	60
2	61	CD4$^+$, CD5$^+$, CD7$^+$, CD10$^+$, BCL6$^+$, PD1$^+$, ICOS$^+$, CXCL13$^+$, EBER$^+$	Lymph node	47,XX,+X,+2,del(6)(q11.1q22.3),+7, der(8)t(8;18)(p11.2;q12.1), der(15) t(15;16)(q26.1;q22.1), der(16)(20q13.3→20p13::16p13.3→p13.1::16p11.1→p13.1::16p13.1→q22.1::15q26.1→q26.3),–18,–20	SYK BA: 2F ITK BA: 2F FER BA: 2F FES BA: 1F1R1G	*TET2*^{H1380Y} *TET2*^{S1449fs}	II	CHOP, remains PET positive	Dead	8
3	83	CD4$^+$, CD2$^-$, CD7$^-$, CD10$^+$, BCL6$^-$, PD1$^+$, ICOS$^+$, CXCL13$^+$, EBER$^+$	Spleen	46,X,–X,der(2)dup(2)(q33.1q33.3) t(2;11)(q37.3;q23.3),t(3;14)(p13;q32.2),del(5)(q14.2q23.2), del(6)(p21.31p24.1),der(8)t(8;8)(p11.21;q22.3),der(11)t(X;11)(q21.1;p15.5),+19	SYK BA: 2F ITK BA: 2F FER BA: 1F FES BA: 2F LSI IGH: 14F, der(3)F	*RHOA*^{G17V} *IDH2*^{R172K} *TET2*^{T1499fs} *TET2*^{Q1687X}	IVBS	Splenectomy plus chlorambucil; progressive disease	Dead	1
4	71	CD3$^+$, CD4$^+$, CD5$^+$, CD23$^+$/ FDC, PD1$^+$, CXCL13$^+$, ICOS$^+$, CD10p$^+$, BCL6w$^+$, EBER$^+$	Lymph node	46,XX	SYK BA: 2F ITK BA: 2F FER BA: 2F FES BA: 2F	*RHOA*^{G17V} *IDH2*^{R172S} *TET2*^{Q769X} *TET2*^{W1219fs} *DNMT3A*^{R771P}	III	CHOP; CR	Alive	160
5	58	CD3$^+$, CD4$^+$, CD5$^+$, CD7$^-$, CD10$^-$, PD1$^+$, ICOS$^+$, BCL6$^+$, CXCL13$^+$, CD21$^+$/ FDC, EBER$^+$	Lymph node	46,XX	SYK BA: 2F ITK BA: 2F FER BA: 2F FES BA: 2F	*RHOA*^{G17V} *IDH2*^{R172S} *TET2*^{N1714fs} *TET2*^{K1752fs}	IIIS	CHOP; CR	Alive	111
6	76	CD3$^+$, CD4$^+$, PD1$^+$, ICOS$^+$, CXCL13$^+$, CD10$^+$, BCL6$^+$, CD23$^+$/FDC, EBER$^+$	Lymph node	47,XX,+5	SYK BA: 2F ITK BA: 3F FER BA: 3F FES BA: 2F	*RHOA*^{G17V} *IDH2*^{R172M} *TET2*^{Y1294C}	IIIS	CHOP; CR	Alive	20

BA, break-apart; CHOP, cyclophosphamide, doxorubicin, vincristine, and prednisone; CR, complete remission; F, fused signal; FDC, follicular dendritic cell; G, green signal; NA, not available; NF, not found; NI, not informative because of a poor resolution of signals on inv(5); NR, no response; p, partial; PET, positron emission tomography; PR, partial response; R, red signal; Rl, relapse; RT, radiotherapy; w, weak.

*Corrected after FISH and array comparative genomic hybridization studies (data not shown).

†Staging according to Ann Arbor.

these can drive FTCL in the absence of *RHOA* mutations. Importantly, we showed that TFH-derived lymphoma can be driven by oncogenic activation of the STAT3 axis. Given that PTKs are amenable for targeted therapy and that murine RHOA-driven lymphomas are responsive to the PI3K inhibitor duvelisib[21] and the mTOR inhibitor everolimus,[22] the use of new therapeutic agents in FTCL should be considered.

Acknowledgments

The authors thank Kathleen Doms, Ursula Pluys, Kim Rummens, and Vanessa Vanspauwen for their excellent technical assistance and Rita Logist for editorial help.

This study was supported by the concerted action grant from the Katholieke Universiteit Leuven No. 3M040406 (J.-A.v.d.K., P.V., T.T., J.C., and I.W.). K.D. was supported by an aspirant fellowship of Fonds voor Wetenschappelijk Onderzoek-Vlaanderen. T.T. holds a Mandate for Fundamental and Translational Research from the "Stichting tegen Kanker" (2°14-083). D.D. holds a Mandate for Clinical and Translational Research from "Kom op tegen Kanker" and for Clinical Research from the University Hospitals Leuven. P.V. is a senior clinical investigator of the Fonds voor Wetenschappelijk Onderzoek-Vlaanderen.

Authorship

Contribution: K.D., J.-A.v.d.K., T.T., J.C., and I.W. designed and performed the research, analyzed the data, and wrote the manuscript; J.A.F.F., K.V.R., L. Marcelis, and G.A. performed research and analyzed data; C.G., D.D., P.V., and L. Michaux provided and analyzed clinical data; and all authors reviewed and approved the manuscript.

Conflict-of-interest disclosure: The authors declare no competing financial interests.

ORCID profiles: G.A., 0000-0002-5838-2879; L. Michaux, 0000-0002-5446-1801; J.C., 0000-0001-6626-5843.

Correspondence: Iwona Wlodarska, Center for Human Genetics, Herestr 49, B-3000 Leuven, Belgium; e-mail: iwona.wlodarska@uzleuven.be.

Footnotes

*K.D. and J.-A.v.d.K. contributed equally to this work.

RNA-seq data are available at Gene Expression Omnibus (Accession No. GSE57944 for patients 1 to 3; pending for patients 4 to 6).

The online version of this article contains a data supplement.

REFERENCES

1. Swerdlow SH, Campo E, Harris NL, et al. *WHO Classification of Tumours of Haematopoietic and Lymphoid Tissues*. 4th ed. Lyon, France: IARC; 2017.
2. Huang Y, Moreau A, Dupuis J, et al. Peripheral T-cell lymphomas with a follicular growth pattern are derived from follicular helper T cells (TFH) and may show overlapping features with angioimmunoblastic T-cell lymphomas. *Am J Surg Pathol*. 2009;33(5):682-690.
3. Streubel B, Vinatzer U, Willheim M, Raderer M, Chott A. Novel t(5;9)(q33;q22) fuses ITK to SYK in unspecified peripheral T-cell lymphoma. *Leukemia*. 2006;20(2):313-318.
4. Dobay MP, Lemonnier F, Missiaglia E, et al. Integrative clinicopathological and molecular analyses of angioimmunoblastic T-cell lymphoma and other nodal lymphomas of follicular helper T-cell origin. *Haematologica*. 2017;102(4):e148-e151.
5. Dierks C, Adrian F, Fisch P, et al. The ITK-SYK fusion oncogene induces a T-cell lymphoproliferative disease in mice mimicking human disease. *Cancer Res*. 2010;70(15):6193-6204.
6. Pechloff K, Holch J, Ferch U, et al. The fusion kinase ITK-SYK mimics a T cell receptor signal and drives oncogenesis in conditional mouse models of peripheral T cell lymphoma. *J Exp Med*. 2010;207(5):1031-1044.
7. Fukumoto K, Nguyen TB, Chiba S, Sakata-Yanagimoto M. Review of the biologic and clinical significance of genetic mutations in angioimmunoblastic T-cell lymphoma. *Cancer Sci*. 2018;109(3):490-496.
8. Fathi NN, Mohammad DK, Görgens A, et al. Translocation-generated ITK-FER and ITK-SYK fusions induce STAT3 phosphorylation and CD69 expression. *Biochem Biophys Res Commun*. 2018;504(4):749-752.
9. Galkin AV, Melnick JS, Kim S, et al. Identification of NVP-TAE684, a potent, selective, and efficacious inhibitor of NPM-ALK. *Proc Natl Acad Sci U S A*. 2007;104(1):270-275.
10. Hellwig S, Miduturu CV, Kanda S, et al. Small-molecule inhibitors of the c-Fes protein-tyrosine kinase. *Chem Biol*. 2012;19(4):529-540.
11. Van Roosbroeck K, Cools J, Dierickx D, et al. ALK-positive large B-cell lymphomas with cryptic SEC31A-ALK and NPM1-ALK fusions. *Haematologica*. 2010;95(3):509-513.
12. Atak ZK, Gianfelici V, Hulselmans G, et al. Comprehensive analysis of transcriptome variation uncovers known and novel driver events in T-cell acute lymphoblastic leukemia. *PLoS Genet*. 2013;9(12):e1003997.
13. Chen ZH, Yu YP, Tao J, et al. MAN2A1-FER fusion gene is expressed by human liver and other tumor types and has oncogenic activity in mice. *Gastroenterol*. 2017;153(4):1120-1132.e15.
14. Boddicker RL, Razidlo GL, Dasari S, et al. Integrated mate-pair and RNA sequencing identifies novel, targetable gene fusions in peripheral T-cell lymphoma. *Blood*. 2016;128(9):1234-1245.
15. Greer PA, Kanda S, Smithgall TE. The contrasting oncogenic and tumor suppressor roles of FES. *Front Biosci (Schol Ed)*. 2012;4(2):489-501.
16. Olvedy M, Tisserand JC, Luciani F, et al. Comparative oncogenomics identifies tyrosine kinase FES as a tumor suppressor in melanoma. *J Clin Invest*. 2017;127(6):2310-2325.
17. Roncagalli R, Cucchetti M, Jarmuzynski N, et al. The scaffolding function of the RLTPR protein explains its essential role for CD28 co-stimulation in mouse and human T cells. *J Exp Med*. 2016;213(11):2437-2457.
18. Zwolak A, Yang C, Feeser EA, Ostap EM, Svitkina T, Dominguez R. CARMIL leading edge localization depends on a non-canonical PH domain and dimerization. *Nat Commun*. 2013;4(1):2523.
19. Greer P. Closing in on the biological functions of Fps/Fes and Fer. *Nat Rev Mol Cell Biol*. 2002;3(4):278-289.
20. King C. New insights into the differentiation and function of T follicular helper cells. *Nat Rev Immunol*. 2009;9(11):757-766.
21. Cortes JR, Ambesi-Impiombato A, Couronné L, et al. RHOA G17V induces T follicular helper cell specification and promotes lymphomagenesis. *Cancer Cell*. 2018;33(2):259-273.e7.
22. Ng SY, Brown L, Stevenson K, et al. RhoA G17V is sufficient to induce autoimmunity and promotes T-cell lymphomagenesis in mice. *Blood*. 2018;132(9):935-947.
23. Uhlén M, Fagerberg L, Hallström BM, et al. Proteomics. Tissue-based map of the human proteome. *Science*. 2015;347(6220):1260419.
24. Crescenzo R, Abate F, Lasorsa E, et al; European T-Cell Lymphoma Study Group. Convergent mutations and kinase fusions lead to oncogenic STAT3 activation in anaplastic large cell lymphoma. *Cancer Cell*. 2015;27(4):516-532.

DOI 10.1182/blood.2019002401